The $\Delta^{17}O$ and $\delta^{18}O$ values of atmospheric nitrates simultaneously collected downwind of anthropogenic sources – Implications for polluted air masses

Martine M. Savard[1*], Amanda Cole[2], Robert Vet[2], Anna Smirnoff[1]

[1] Geological Survey of Canada (Natural Resources Canada), 490 de la Couronne, Québec (QC), G1K 9A9, Canada
[2] Air Quality Research Division, Environment and Climate Change Canada, 4905 Dufferin St., Toronto (ON), M3H 5T4, Canada

Correspondence to: Martine M. Savard (martinem.savard@canada.ca)

Abstract. There are clear motivations for better understanding the atmospheric processes that transform nitrogen (N) oxides (NO_x) emitted from anthropogenic sources into nitrates (NO_3^-), two of them being that NO_3^- contributes to acidification and eutrophication of terrestrial and aquatic ecosystems, and particulate nitrate may play a role in climate dynamics. For these reasons, oxygen isotope delta values ($\delta^{18}O$, $\Delta^{17}O$) are frequently applied to infer the chemical pathways leading to the observed mass independent isotopic anomalies from interaction with ^{17}O-rich ozone (O_3). Recent laboratory experiments suggest that the isotopic equilibrium between NO_2 (the main precursor of NO_3^-) and O_3 may take long enough under certain field conditions that nitrates may be formed near emission sources with lower isotopic values than those formed further downwind. Indeed, previously published field measurements of oxygen isotopes in NO_3^- in precipitation (w-NO_3^-) and in particulate (p-NO_3^-) samples suggest that abnormally low isotopic values might characterize polluted air masses. However, none of the air studies have deployed systems allowing collection of samples specific to anthropogenic sources in order to avoid shifts in isotopic signature due to changing wind directions, or separately characterized gaseous HNO_3 with $\Delta^{17}O$ values. Here we have used a wind-sector-based, multi-stage filter sampling system and precipitation collector to simultaneously sample HNO_3 and p-NO_3^-, and co-collect w-NO_3^-. The nitrates are from various distances (<1 to >125 km) downwind of different anthropogenic emitters, and consequently from varying time lapses after emission.

The separate collection of nitrates shows that the HNO_3 $\delta^{18}O$ ranges are distinct from those of w- and p-NO_3^-. Interestingly, the $\Delta^{17}O$ differences between p-NO_3^- and HNO_3 shift from positive during cold sampling periods to negative during warm periods. The low p-NO_3^- $\Delta^{17}O$ values observed during warm periods may partly derive from the involvement of ^{17}O-depleted peroxy radicals (RO_2) oxidizing NO during that season. Another possibility is that nitrates derive from NO_x that has not yet reached isotopic equilibrium with O_3. However, these mechanisms, individually or together, cannot explain the observed p-NO_3 minus HNO_3 isotopic changes. We propose differences in dry depositional rates, faster for HNO_3, as a mechanism for the observed shifts. Larger proportions of p-NO_3^- formed *via* the N_2O_5 pathway would explain the opposite fall-winter patterns. Our results show that the separate HNO_3, w-NO_3^- and p-NO_3^- isotopic signals can be used to further our understanding of NO_x oxidation and deposition. Future research should investigate all tropospheric nitrate species as well as NO_x to refine our understanding of nitrate distribution worldwide and to develop effective emission reduction strategies.

1 Introduction

Anthropogenic NO_x (NO and NO_2) emissions are oxidized to nitrate in the atmosphere in the form of gaseous, wet or particulate forms, HNO_3 being one of the main precursors of p-NO_3^-. All these species may have detrimental effects on human health and aquatic and terrestrial ecosystems through inhalation, acidification and excess nitrogen deposition. In addition, aerosols may play a significant role in regional climate dynamics as they interact with clouds and solar radiation (e.g., IPCC, 2013). For these reasons, understanding the chemical processes controlling the transport and fate of atmospheric reactive N is required to help develop effective emission reduction strategies and drive climate models (in the present article, we use *nitrates* to collectively refer to p-NO_3, HNO_3 and w-NO_3).

Triple oxygen isotopes ($\delta^{18}O$ and $\delta^{17}O$) have been used to decipher atmospheric oxidation pathways of NO_x leading to ambient nitrate. Michalski et al. (2003) performed the first measurement of $\delta^{17}O$ values in atmospheric nitrate. The authors found nitrate highly enriched in ^{18}O and ^{17}O, likely due to the transfer of anomalous oxygen atoms from ozone (O_3) via the NO_x-ozone photochemical cycle and oxidation to nitrate. During its formation, O_3 inherits abnormally high $\delta^{18}O$ and $\delta^{17}O$ values through mass independent fractionation. The specific $\delta^{17}O$ departure from the terrestrial mass dependent fractionation line, named the ^{17}O anomaly, is often expressed as $\Delta^{17}O = \delta^{17}O - 0.517 \times \delta^{18}O$ (Thiemens, 1999). Further investigations suggested that the $\delta^{18}O$ and $\delta^{17}O$ values of w-NO_3^- and p-NO_3^- reflect several reactions taking place after the atmospheric emission of NO_x, *i.e.*, atmospheric oxidation pathways transforming NO_x into secondary products (Hastings et al., 2003; Michalski et al., 2003; Michalski et al., 2004; Morin et al., 2007; Savarino et al., 2007; Alexander et al., 2009). Seasonal $\delta^{18}O$ differences in w-NO_3^- samples (less variable and lower values during summer) have been interpreted to be due to changes in these chemical pathways (Hastings et al., 2003). Modeling and validation based on sparse existing data provide hope regarding a global understanding of atmospheric nitrate (Alexander et al., 2009), however, further measurements need to be done on the ground, particularly at mid-latitudes.

Additional studies dealing with triple oxygen isotope characterizations have addressed questions of methodology (Kaiser et al., 2007; Smirnoff et al., 2012), transfer of the ozone ^{17}O anomaly to atmospheric nitrate (Liang and Yung, 2007; Savarino et al., 2008; Michalski et al., 2014), or sources and chemical pathways of high (Arctic) and low (Taiwan) latitude nitrate (Morin et al., 2008; Guha et al., 2017, respectively). Triple oxygen isotope characterizations of field NO_3^- samples are not yet widespread. Also rare are the nitrate $\delta^{18}O$ and $\Delta^{17}O$ values of field samples downwind from NO_x-emitting sources at mid-latitudes (Kendall et al., 2007; Proemse et al., 2013). The few existing studies have chiefly characterized w-NO_3^- or the sum of p-NO_3^- and HNO_3 (Michalski et al., 2004; Morin et al., 2007; Morin et al., 2008; Alexander et al., 2009; Morin et al., 2009; Proemse et al., 2012; Guha et al., 2017), and suggested these indicators would be useful to trace atmospheric nitrate in water (Kendall et al., 2007; Tsunogai et al., 2010; Dahal and Hastings, 2016), or to apportion the contribution of anthropogenic emissions to regional atmospheric nitrate loads (Proemse et al., 2013).

In the past, due to sampling challenges, HNO_3 and p-NO_3^- were generally collected together (without differentiation). Therefore, no studies have separately and simultaneously collected and analyzed the HNO_3 and p-NO_3^- $\delta^{18}O$ and $\Delta^{17}O$ values, and discussed these isotopic characteristics of nitrate collected downwind of anthropogenic emitters. While HNO_3 and p-NO_3^- can be in equilibrium (e.g. if p-NO_3^- is in the form of solid NH_4NO_3), this is not always the case, for example, if nitrate is

bonded to calcium or dissolved in liquid water on a wet particle (see section 3.3). They have different lifetimes with respect to wet scavenging (Cheng and Zhang, 2017) and dry deposition velocities (Zhang et al., 2009), and may differ in their formation pathways as well. Therefore, investigating the mass independent and dependent oxygen fractionations in nitrates separately collected may help identifying their respective formation and loss pathways, and provide additional constraints on processes controlling their distribution.

Here we have characterized nitrate collected downwind of five emission sources in central and southern Alberta, Canada, namely: (1) coal-fired power plants, (2) city traffic, (3) chemical industries and metal refining, (4) fertilizer plant and oil refinery, and (5) gas compressors plus cattle and swine feedlots. To this end, we employed wind-sector-based active samplers to collect HNO_3 and p-NO_3^- as well as w-NO_3^- downwind of the source types. The objective of this work was to assess the atmospheric NO_x reaction pathways and determine processes responsible for the distribution of HNO_3, and w- and p-NO_3^- in a mid-latitudinal region.

2 Methodology

2.1 Regional context

While national reported NO_x emissions in Canada declined steadily from 2000 to 2015, emissions in the Province of Alberta have remained relatively constant since 2004 (Environment and Climate Change Canada, 2016). Pioneering work was accomplished measuring nitrate on emitted PM2.5 (particulate matter less than 2.5 μm) and in bulk and throughfall precipitation samples (wet and some dry deposition on ion exchange resin collectors) collected at or downwind of the Athabasca oil-sands mining operations in northern Alberta (Proemse et al., 2012; Proemse et al., 2013). However, the Edmonton area in central Alberta, known to generate the highest NO_x emissions in Canada, and the area of southern Alberta, characterized by dense gas compressor station and agricultural emissions, have never been investigated.

This research project investigated nitrates (p-NO_3^-, HNO_3 and w-NO_3^-) from two main emission source areas: the Genesee and Edmonton areas of central Alberta, and the Vauxhall area of southern Alberta (Fig. 1A). These areas experience a continental climate, but the mean annual temperature at Vauxhall is slightly higher (5.6 °C) and total annual precipitation lower (320 mm) than in central Alberta (3.9°C; 537 mm; Fig. SM-1). Autumn is generally the wettest season and winter the driest. The sampling sites were at altitudes between 645 and 820 m (altitude above sea level), and in continental regions devoid of the influence of marine air masses (negligible halogen oxides).

The rural Vauxhall area was selected for collecting nitrates emitted from multiple small gas compressor stations scattered throughout southern Alberta and reduced N from cattle and swine feedlots. The other anthropogenic emissions are from three sites in central Alberta (Fig. 1B): coal-fired power plants (CFPP) at the Genesee site, 55 km southwest of Edmonton; traffic-dominated emissions at Terrace Heights, a residential area near downtown Edmonton; and an industrial area in Fort Saskatchewan, northeast of Edmonton, where sampling two different wind sectors allowed separating different industries. In

Fort Saskatchewan, sampling in the northwest sector targeted emissions from a mixture of sources of which the largest were a chemical plant and metal refinery (referred to as chemical plus metal industries; distance to sources of 3 to 7 km), while the north sector point emissions were dominated by a fertilizer plant and an oil refinery (referred to as fertilizers plus oil; distance to sources from 9 to 14 km). The NO_x emissions reported to the National Pollutant Release Inventory (Environment and Climate Change Canada, 2018b) for 2013 from all Alberta sources are also shown in Fig. 1.

2.2 Sampling protocols

Collection of nitrate samples took place between 30 September 2010 and 20 January 2014. Active air sampling was carried out using a modified version of Environment Canada's CAPMoN (Canadian Air and Precipitation Monitoring Network) sampling protocol, which is described in detail elsewhere (Sirois and Fricke, 1992). Precipitation sampling also followed CAPMoN wet-only protocols as described in the literature (Sirois and Vet, 1999). A 'conditional sampling' method was employed to maximize the collection of nitrogen compounds from the anthropogenic sources, in which the sampling pumps and precipitation collector were activated when the site wind vane registered winds faster than 0.55 m/s (2 km/h) from the direction of the targeted sources. The CAPMoN sampling system was installed and operated at different sites, each at varying distances from the targeted point (<1 to 35 km), and diffuse sources (3 to >125 km; Table 1). Back trajectories run using the HYSPLIT model (Stein et al., 2015; Rolph, 2017) for every hour of sampling verified that the conditional sampling approach collected air masses that had primarily passed over or near the targeted source (i.e., there was no landscape feature that decoupled wind direction from back trajectories; see sample plot of back trajectories from Genesee in Fig. SM-2).

Ambient air was pulled through a three-stage filter pack system to collect, sequentially, particulate matter on a Teflon filter, gaseous nitric acid (HNO_3) on a Nylasorb nylon filter, and gaseous ammonia on a citric acid-coated Whatman 41 filter (all 47 mm). The Teflon-nylon filter method for p-NO_3^- and HNO_3 has been extensively compared and evaluated, and is currently used by national monitoring networks targeting regional background sites, CAPMoN in Canada and CASTNet (Clean Air Status and Trends Network) in the United States. Previous testing showed negligible collection of HNO_3 on the Teflon filter, <3% breakthrough of HNO_3 from the nylon filter with loadings more than three times higher than reported here, and blanks for p-NO_3^- and HNO_3 of approximately 0.2 µg N per filter (Anlauf et al., 1985; Anlauf et al., 1986). Intercomparisons with more labor-intensive methods, such as tunable diode laser absorption spectroscopy and annular denuder-filter pack systems, have shown evidence of some volatilization of ammonium nitrate from the Teflon filter leading to a negative bias in p-NO_3^- and positive bias in HNO_3 under hot (> 25 °C) and dry conditions, particularly in high ambient concentrations (e.g., Appel et al., 1981). However, other field studies have shown no significant differences in HNO_3 between filter packs and denuder and/or TDLAS systems (Anlauf et al., 1986; Sickles Ii et al., 1990) or mixed results (Spicer et al., 1982; Zhang et al., 2009). While those studies used short-duration sampling, a comparison for weekly samples at a lower-concentration site showed good agreement between filter pack and denuder values for most of the study but potential interference from HNO_2 (nitrous acid) on the nylon filter in two samples (Sickles Ii et al., 1999). Based on the conditions in Alberta, we estimate that there is little or no volatilization of NH_4NO_3 for samples with mean temperatures below 5 °C, but there is a possibility for nitrate loss of up to 30% in the warmest sampling periods.

After the first five sample periods, an experimental active sampling system for NO_2 and NO_x was added downstream of the three-stage filter pack. This system consisted of one or two custom cartridges packed with Maxxam Analytics' resin to selectively collect NO_2, and one- or two-stage filter pack containing two identical Maxxam Analytics' impregnated filters designed to collect NO_x (mostly NO due to upstream collection of NO_2). Oxygen isotopes in NO_2 and NO_x were not measured since we could not rule out oxygen isotope exchange during the extraction process, however, concentrations meeting the QC criteria (Savard et al., 2017) are presented for reference in Table SM-1.

Here we report on oxygen isotopes in the simultaneously sampled HNO_3 and p-NO_3^-, along with co-sampled w-NO_3^- in rain and snow samples. Note that precipitation events did not occur regularly (see Fig. SM-1), so that the number of aqueous samples collected was fewer than the gas and particulate samples. Both the air and precipitation samplers were only active when the wind direction was from the desired source sector and the wind speed was greater than 0.55 m/s (2 km/h). Four identical air-sampling systems operated simultaneously at each site, with samples pooled when necessary to provide sufficient filter loadings for isotope analysis and, when possible, measured separately to estimate sampling precision. In contrast to the four gas-and-particle sampling systems, there was a single precipitation collector at each site, and therefore external precision was not determined for precipitation samples. Individual sample deployment times ranged from 5 to 113 days, and total air sampling time within the wind-direction sectors ranged from 21 to 360 hours (Table SM-1). The variable cumulative periods reflected the frequency of the wind flow from the targeted source sectors and the amount of time required to obtain sufficient mass loadings on the filters.

Two or three replicate samples for most species were pooled at Genesee and Vauxhall, the first two sampling sites, subject to the requirement that sampled air volumes be within 15 % of each other, thereby eliminating samples that experienced flow problems. Flow issues were primarily due to pump failure, likely caused by cycling the pumps on and off frequently in early samples. Therefore, for later samples the protocol was changed such that the pumps remained on and valves were used to switch the pumps between sampling lines and non-sampling tubing based on the wind sector. At the sites sampled later in the Edmonton area, improvements to the laboratory analytical procedure allowed for smaller sample amounts and eliminated the need for sample pooling.

2.3 Analytical procedures

Nitric acid from nylon filters were extracted using 10 mL of 0.01M solution of NaCl. Particulate-NO_3 from Teflon filters were extracted in two portions of 6 mL of ultrapure water (ELGA). To reduce possible evaporation, filters were placed in an ultrasonic bath with ice. The extractions were performed during one hour and samples were left for 48 hours in a fridge to insure the complete extractions. The solutions were decanted and a small portion (1-2 mL) was used to determine concentrations. The remaining extracts were stored in the fridge for subsequent isotope analysis. The blanks from both filters were treated the same way.

Concentration of nitrates in Teflon and Nylon filter extracts, and in precipitation samples were determined at the Institut national de la recherche scientifique – Eau, Terre, Environnement (INRS-ETE). The determinations used an automated QuikChem 8000 FIA+ analyzer (Lachat Instruments), equipped with an ASX-260 series autosampler. The detection limit for the method with sulfanilamide (# 31-107-04-1-A) was 2 ppb (0.03 μmol/L of NO_3^--N). Nitrite concentrations were also measured in the extracts. Nitrite concentrations above the detection limit (1.14 μmol/L of NO_2^--N) were found in a handful of samples at Terrace Heights. These samples were excluded from the reported data.

We characterized the $\delta^{17}O$, $\delta^{18}O$ and $\delta^{15}N$ ratios of HNO_3, w-NO_3^-, and p-NO_3^-, along with the $\delta^{15}N$ values of NH_3, w-NH_4, p-NH_4 and NO_x (all N isotopic results are in Savard et al., 2017). The present article deals solely with the $\delta^{18}O$ and $\Delta^{17}O$ values obtained for the three nitrate species. We treated the samples using the chemical conversion and thermal decomposition of N_2O protocols, providing the ability to simultaneously analyze low-concentration N- and O-containing species (Smirnoff et al., 2012).

A notable challenge in the analysis of the filter-based atmospheric samples is their small extraction volumes. Only 10-12 mL of extract solution were normally available for the measurement of concentrations and isotopic analysis. In addition, the concentrations of these low volume samples were also low (7.1-21.4 μmol/L of NO_3^--N). Therefore, not all samples could be diluted to produce volumes sufficient for reduction of NO_3^- to NO_2 and subsequent conversion to N_2O, the final product before isotope analysis. Samples with an initial concentration below 2.3 μmol/L could not be treated individually and were combined to produce volumes sufficient for analyses (same sampling period but combination of collected parallel samples).

The preparation steps involved conversion of nitrate-containing samples into nitrite (NO_2^-) using a custom-made cadmium column. The final preparation step involved using sodium azide to ultimately produce N_2O (McIlvin and Altabet, 2005; Smirnoff et al., 2012). All extracted N_2O was analyzed using a pre-concentrator (PreCon, Thermo Finnigan MAT) including a furnace with 'gold' wires, online with an Isotope Ratio Mass Spectrometer (Delta V Plus, Thermo Electron; Kaiser et al., 2007; Smirnoff et al., 2012). The utilized approach allows the spectrum of $\delta^{15}N$, $\delta^{17}O$ and $\delta^{18}O$ values from O-bearing N-species to be determined in samples containing as little as 37.5 nmol of N (15 mL final solution). Extracts from filter blanks were processed in the same way. The blanks from nylon filters were not detectable. Peak heights from the blanks resulting from Teflon filters were detected and always below 10% of sample peaks, having a negligible effect (within the analytical precision). The USGS-34, USGS-35, USGS-32 nitrate reference materials were used and processed exactly the same way as the samples, *i.e.*, converted from nitrate to nitrite, then to N_2O. The laboratory analytical precision (average of replicates) determined during the present study was 0.6 ‰ for $\delta^{18}O$ and $\delta^{17}O$ values in gaseous (n=12) and solid nitrates (n=20). For w-NO_3, analytical replicates gave 0.6 and 0.5 ‰, for $\delta^{18}O$ (n=3) and $\delta^{17}O$ (n=4) values, respectively. The $\Delta^{17}O$ values are defined as $1000 \times \ln(1+\delta^{17}O/1000) - 0.516 \times 1000 \times \ln(1+\delta^{18}O/1000)$, relative to Vienna Standard Mean Ocean Water (VSMOW).

3 Results and interpretation

3.1 Isotopic reproducibility when using the CAPMoN filterpack sampling system

Data obtained from at least two of the four identical CAPMoN sample collection streams at each sampling site were used to calculate the reproducibility of each isotopic value measured. With four or fewer samples collected during each sampling period, a non-parametric approach was deemed most appropriate. Therefore, for each of the 18 sampling periods a median isotopic value was calculated, then the two to four absolute deviations from this median were calculated (Table 2; Table SM-1). Although there were four replicates in 18 periods, the pooling of simultaneously collected samples and the QC steps described earlier reduced the total number of replicates for each compound (Table 3). The median absolute deviation (MAD) for each compound was then calculated from the 15-38 absolute deviations. Finally, for comparability with the more familiar standard deviation, the MAD was scaled using the standard 0.6745 divisor to give the modified median absolute deviation (M.MAD), a scaled parameter that will be equal to the standard deviation in the event that the distribution is Gaussian (Randles and Wolfe, 1979; Sirois and Vet, 1999). This suite of parallel tests indicates that all measured species show coherent and reproducible $\delta^{17}O$ and $\delta^{18}O$ results, with the M.MAD varying between 0.7 and 2 ‰ (Table 2). These estimations encompass the precision of the entire method, including errors due to sampling, chemical treatments and instrumental analysis.

A potential complication of the air sampling method can arise if there was significant volatilization of NH_4NO_3 on the particle filter into HNO_3 and NH_3, with subsequent collection on the downstream gas filters. This could result in equilibrium isotopic fractionation between the particle and gaseous components, which would become artificially high and low, respectively, with more fractionation at higher temperatures (summer) relative to lower temperatures (winter) when volatilization is minimal (Keck and Wittmaack, 2005). We find the p-NO_3^- isotopic values ($\delta^{17}O$ and $\delta^{18}O$) to be generally higher during winter than during summer (see sub-section 3.4). Moreover, the p-NO_3^- $\delta^{18}O$ minus HNO_3 $\delta^{18}O$ differences are negative during summer (see sub-section 3.6), opposite to the expected isotopic artefact if particulate volatilization were the dominant factor in determining the particle-gas isotopic differences (the same was concluded for the $\delta^{15}N$ values in NH_3 and NH_4; Savard et al., 2017). We therefore conclude that, while volatilization may occur in the summer samples, other isotope effects must be larger in order to lead to the observed differences. In addition, volatilization would cause mass-dependent fractionation and would not affect the ^{17}O anomaly; therefore, $\Delta^{17}O$ values remain robust indicators of chemical pathways in this situation. Finding that the sampling protocols are adequate for isotopic work is in agreement with a previous study using a comparable method that found minimal fractionation for p-NO_3^- and HNO_3 (Elliott et al., 2009).

3.2 Concentrations and isotopic ratios of nitrates in Alberta samples

The range of HNO_3-N concentrations measured by the filters (from 0.01 to 0.15 μg/m^3; average of 0.06) are slightly lower than those of p-NO_3^--N (from 0.02 to 0.35 μg/m^3; average of 0.12). For context, the median concentrations at all CAPMoN sites, which represent non-urban areas across Canada, range from 0.02 to 0.25 μg/m^3 for HNO_3-N and from 0.007 to 0.45 μg/m^3 for p-NO_3^--N (Cheng and Zhang, 2017), with the higher values at sites affected by regional and transboundary pollution. Background sites for this region are sparse, but concentrations at Cree Lake in neighbouring Saskatchewan were the lowest in Canada reported up to 2011 (Cheng and Zhang, 2017), and 2014-2016 measurements at Wood Buffalo National Park on the

northern Alberta border revealed similar average concentrations of 0.02 μg/m^3 of NO_3^--N for both HNO_3 and p-NO_3^- (preliminary internal data). Therefore, the lowest concentrations in our samples approached average background concentrations, while the highest were 20 or more times higher than regional background. The range of NO_3^--N concentrations of the w-NO_3^- samples was 0.15 – 0.48 mg/L. For comparison, volume-weighted mean annual concentrations of nitrate at the remote CAPMoN site to the north (Snare Rapids) for 2011-2014 were approximately 0.07 mg/L of NO_3^--N, while at the most polluted site in southern Ontario (Longwoods) the volume-weighted mean concentration was approximately 0.3 mg/L (Environment and Climate Change Canada, 2018a). It should be pointed out that precipitation ion concentrations vary significantly with precipitation amount, so the short samples collected here are not necessarily representative of annual volume-weighted means.

The average $\delta^{18}O$ and $\Delta^{17}O$ values of HNO_3 (gas), w- and p-NO_3^- show no apparent systematic ordering (Table 3; Tables SM-1 and 2), in contrast to what was found for $\delta^{15}N$ values in the same samples (Savard et al., 2017). As expected, there is no systematic tendency when looking at the samples collected from the anthropogenic sources: CFPP HNO_3 and p-NO_3^- have the highest $\delta^{18}O$ and $\Delta^{17}O$ averages, but not the highest delta values for w-NO_3^- values; chemical industries show the lowest $\delta^{18}O$ and $\Delta^{17}O$ averages for w- and p-NO_3, but not for HNO_3. Though the number of samples were limited, w-NO_3^- $\Delta^{17}O$ values were roughly correlated with the weighted average $\Delta^{17}O$ values of p-NO_3 and HNO_3 in samples covering the same time periods, consistent with scavenging of both HNO_3 and p-NO_3 by wet deposition. This observation indicates that the oxygen isotopes in the three nitrate species are not predominantly source dependent (see also Fig. SM-3), as previously suggested in the literature (Michalski et al., 2003).

Considering all nitrate species, the Alberta $\delta^{18}O$ and $\Delta^{17}O$ values range between +48.4 and +83.2 ‰, and between 13.8 and 30.5 ‰, respectively (Table 4; Table SM-1, Fig. SM-4). These ranges indicate that ozone partly transferred its isotopic anomaly to nitrates during NO_x cycling and oxidation (nitrate derived through combustion in O_2 would show $\delta^{18}O$ and $\Delta^{17}O$ values of 23.5 and 0 ‰, respectively). When examining the existing $\delta^{18}O$ and $\Delta^{17}O$ data for w- and p-NO_3^- in the literature, the ranges for our mid-latitude samples are within those previously reported (Table 4). The worldwide compilation of documented data is broadening the $\delta^{18}O$ range of atmospheric NO_3^- previously suggested to be between 60 and 95 ‰ (Hastings et al., 2003; Kendall et al., 2007).

Previous studies that report triple isotope oxygen results in atmospheric NO_3^- samples are scarce (Table 4). The HNO_3 range documented here is within the broad spectrum of p-NO_3^- values compiled for remote to contaminated sites. Elliott et al. (2009) reported HNO_3 oxygen results for $\delta^{18}O$ values only, with a range of +51.6 to +94.0 ‰ (mean of 77.4), with simultaneously-sampled p-NO_3^- $\delta^{18}O$ values between +45.2 and +92.7 ‰ (mean of 75.2). Those ranges are broader than the HNO_3 and p-NO_3^- values obtained in the present study.

3.3 The $\delta^{18}O$ and $\Delta^{17}O$ trends in nitrates from cold and warm sampling periods

The $\delta^{18}O$ and $\Delta^{17}O$ ranges for HNO_3 identified by sampling period are narrower than those of the simultaneously collected p-NO_3^- (Fig. 2; Table SM-1), suggesting that there are additional mechanisms affecting HNO_3, or that p-NO_3 is derived from

different pathways with more variation in isotopic signatures. Overall, the $\Delta^{17}O$ and $\delta^{18}O$ results for HNO_3, w-NO_3^- and p-NO_3^- clearly show higher $\delta^{18}O$ and $\Delta^{17}O$ values during cold periods relative to warm periods (Fig. 2), with the exception of HNO_3 $\delta^{18}O$ values, which were similar in cold and warm periods. The collection of several samples lasted over periods overlapping fall and winter and, in such cases, the results are labelled as covering the two seasons; note that for many fall cases, the average sampling temperatures were below 0 ºC (Table SM-3). Nevertheless, plotting by sampling period can be regarded as a general repartition of results between warm and cold months, which show lower and higher isotopic values, respectively, in both the w- and p-NO_3^-.

A series of reactions listed in Table 5 summarizes the main atmospheric processes taking place during the production of nitrates in contaminated air masses. First, during anthropogenic combustion of fossil fuels, NO_x (NO and NO_2) is produced through reactions of air N_2 with atmospheric O_2 at high temperatures (reactions R1; Table 5). Then, NO_x cycles between NO and NO_2 through a series of reactions involving sunlight (R5), O_3 (R2, R4), and peroxy (HO_2) or alkyl peroxy (RO_2) radicals (R3; Morin et al., 2007; Fang et al., 2011; Michalski et al., 2014; here we use RO_2 to refer collectively to HO_2 and RO_2).

The oxidation of NO_x (specifically NO_2) to HNO_3 further incorporates additional O atoms from different oxidants (R6-R8; Table 5). Production of nitrate via R6 is restricted to daytime (since OH is generated through photochemistry), whereas production through reactions R4, R7 and R8 dominates at night. In addition, N_2O_5 is thermally unstable, so the contribution of the R4-R7-R8 pathway is larger during winter than during summer. Additionally, in the heterogeneous hydrolysis of N_2O_5 (R8), HNO_3 is likely to be retained on the reaction particle as p-NO_3^- due to its hygroscopicity (Seinfeld and Pandis, 2006). We have neglected contributions from BrO cycling due to the location far from the coast, and from reactions of NO_3 with hydrocarbons (R12) since they are predicted to have a minimal contribution to nitrate formation in this region (Alexander et al., 2009). Finally, HNO_3 in the gas phase can be irreversibly scavenged by wet surfaces or precipitation (R9) and calcium carbonate on particles (R11), and can equilibrate with solid ammonium nitrate where there is excess ammonia available (R10).

It has been previously suggested that the $\delta^{18}O$ and $\Delta^{17}O$ values of w- and p-NO_3^- formed during summer are lower than those during winter due to higher contribution from the N_2O_5 path (R4, R7-R8) during that season (e.g., Hastings et al., 2003; Morin et al., 2008). As an early take on the data identified by sampling periods, the w- and p-NO_3^- $\delta^{18}O$ and $\Delta^{17}O$ data presented here follow the same patterns for warm and cold months (Fig. 2). In contrast, the less commonly studied HNO_3 shows similar $\delta^{18}O$ values during warm and cold seasons, but summer $\Delta^{17}O$ values mostly lower than the fall-winter, fall and spring ones.

3.4 Correlations with meteorological parameters and co-pollutants

The distribution and proportion of HNO_3 and p-NO_3^- in polluted air masses can vary daily and seasonally with temperature, relative humidity (RH) and concentration of co-contaminants (Morino et al., 2006). For that reason, we compared the isotopic ratios of the HNO_3 and p-NO_3 samples (n of w-NO_3 too low) with meteorological and air quality parameters measured routinely at nearby monitoring stations where available (Table SM-3). We found that the p-NO_3^- and HNO_3 $\delta^{18}O$ and $\Delta^{17}O$ values correlate with RH, with p-NO_3 values showing stronger statistical links than HNO_3 (Table 6). The N_2O_5 hydrolysis reaction (R8) rate increases with humidity (Kane et al., 2001), which may explain this positive correlation. Significant inverse

relationships exist between temperature and p-NO_3^- $\delta^{18}O$, p-NO_3^- $\Delta^{17}O$, and HNO_3 $\Delta^{17}O$. These negative links likely arise since N_2O_5 is more stable under cold conditions, leading to a higher contribution of R8. The stronger links with p-NO_3^- may be due to R8 taking place on surfaces (such as particles) with liquid water, which is likely to retain the HNO_3 as p-NO_3^- rather than release it to the gas phase. Therefore, in winter, R8 may contribute more to p-NO_3^- than to HNO_3(g). Moreover, the highest $\delta^{18}O$ and $\Delta^{17}O$ values for both p-NO_3^- and HNO_3 were found for fall-winter samples collected at high RH (76 %) and low temperature (-10°C). In contrast, the lowest p-NO_3^- isotopic values were found for samples with similar proportions of HNO_3 and p-NO_3^-, and sampled during moderately humid (60-63 %) and warm (8-20°C) periods. The accompanying shift in $\delta^{18}O$ and $\Delta^{17}O$ differences between p-NO_3 and HNO_3, will help infer the mechanisms dominating during the cold and warm periods (Section 4.2).

Concentrations of oxidants, co-contaminants (e.g., SO_4^- aerosols) and NO_x influence the dominance and rates of the discussed reactions (Brown et al., 2006; Michalski et al., 2014). However, while temperature, RH and O_3 are well captured within a 5 km radius, other pollutant measurements like continuous SO_2, $PM_{2.5}$ and NO_x can have large gradients near sources, therefore it is not surprising that no correlations were found with SO_2 or $PM_{2.5}$ measured at sites 4-5 km away (Table 6). Surprisingly, only the p-NO_3^- $\Delta^{17}O$ and $\delta^{18}O$ values correlated with the fraction of each sample collected during daylight hours (i.e., between the sunrise and sunset times on the day at the middle of each sampling period, either at Edmonton or Lethbridge), which was expected for HNO_3 as well due to the daytime-only OH pathway. However, daylight hours do not take into account light intensity, which can influence significantly the oxidation rate through this pathway, and consequently both the $\delta^{18}O$ and $\Delta^{17}O$ values.

3.5 Comparison with high-latitude p-NO_3^-

An interesting aspect of the Alberta p-NO_3^- cold-period $\Delta^{17}O$ ranges is that they compare relatively well with the range obtained for the Canadian Arctic (Fig. 4), during winter, when nighttime conditions and the N_2O_5 pathway prevail without interruption (Morin et al., 2008; for comparison with HNO_3 values see Fig. SM-4). This observation supports the suggestion that the N_2O_5 pathway produces around 90 % of nitrates during mid-latitudinal cold months (Michalski et al., 2003; sub-section 4.1). The $\delta^{18}O$ ranges of cold months are similar in Alberta and in the Arctic. This similarity goes against previous suggestions that at higher latitudes, nitrate $\delta^{18}O$ annual means should be higher than at mid-latitudes due to local ambient conditions and atmospheric chemistry affecting the proportions of species involved in producing nitrate (Morin et al., 2009), namely, the sole influence of the N_2O_5 pathway during the Arctic winter (Fang et al., 2011).

The $\Delta^{17}O$ departure between the Alberta and Arctic winter parallel lines is about 3 ‰. Such difference is slightly larger than the one calculated for winter NO_3^- at 80 and 40° N latitudes (about 2 ‰; Morin et al., 2008). In contrast, the warm-months and summer data sets for Alberta and the Arctic, respectively, show different isotopic ranges (Fig. 5), possibly due to the plume effects described later (sub-section 4.3). Moreover, contrary to a previous suggestion, the winter-summer difference in nitrate $\Delta^{17}O$ values is similar at the mid- and high-latitudinal sites (about 6 ‰ here, and 5 ‰ in Morin et al., 2008). This similarity is likely coincidental as it may reflect the fact that within-plume chemistry may lower the $\Delta^{17}O$ values of NO_x in the sampled anthropogenic plumes in Alberta (see sub-section 4.3 for details), whereas the seasonal departure in Arctic samples comes from

the oxidation to nitrate through the dominant OH and N_2O_5 pathways during summer and winter, respectively. Finally, the $\Delta^{17}O$ averages for the Alberta summer and winter results approximately fits within ranges predicted for the studied area by global modeling (Alexander et al., 2009), suggesting that global modeling of nitrate distribution worldwide is promising.

3.6 Isotopic differences between HNO_3 and p-NO_3^-

As far as the isotopic characteristics are concerned, an important feature to keep in mind is that the HNO_3 of central and southern Alberta has distinct properties relative to simultaneously sampled p-NO_3^-. In practical terms, the relationships between the simultaneously sampled HNO_3 and p-NO_3^- are of four types (Fig. 3): (i) HNO_3 $\delta^{18}O$ and $\Delta^{17}O$ are both lower than p-NO_3^-; (ii) HNO_3 has lower $\Delta^{17}O$ but higher $\delta^{18}O$ values than p-NO_3^-; (iii) HNO_3 has higher $\delta^{18}O$ values and similar $\Delta^{17}O$ ones relative to p-NO_3^-; and (iv) HNO_3 has higher $\delta^{18}O$ and $\Delta^{17}O$ values than p-NO_3^- (Fig. 3).

The fall-winter isotopic results belong to group (i), fall results, to groups (i), (ii) and (iii), and the spring and summer results, to groups (ii), (iii) and (iv) (Fig. 3). Elliott et al. (2009) reported simultaneously sampled p-NO_3^- and HNO_3 in northeastern USA with similar seasonal changes of $\delta^{18}O$ differences (no $\Delta^{17}O$ measurement). The HNO_3 $\delta^{18}O$ were generally similar or lower than the p-NO_3^- values during winter and fall, and slightly to much higher during spring and summer, with the spring and autumn p-NO_3^--HNO_3 relationships being roughly intermediate between the winter and summer ones. The average $\delta^{18}O$ difference of p-NO_3^- minus HNO_3 reported between winter and summer (15 ‰) by Elliott et al. (2009) agrees with the difference for fall-winter and summer obtained here (12 ‰).

The marked shifts in isotopic differences between the separately analyzed HNO_3 and p-NO_3^- reported here likely reflect changes in the dominant reactions and processes leading to the production of the two nitrates (see sub-section 4.2). Analyzing them separately provides additional granularity that may be used to elucidate further details of the production and loss of nitrate species downwind from a NO_x source.

4 Discussion

4.1 Estimation of $\Delta^{17}O$ values of NOx precursor to the studied nitrates- Highlighting oxidation mechanisms

In the present sub-section, we estimate the $\Delta^{17}O$ values of NO_2 involved during the production of the Alberta nitrates based on the observed nitrate values and discuss the implications of these estimations. Generally, winter to summer isotopic differences are thought to be due to the high oxygen isotopic values of N_2O_5 due to interaction with O_3 (Johnston and Thiemens, 1997; Michalski et al., 2003; Morin et al., 2008; Vicars et al., 2012) and low values of OH in isotopic equilibrium with atmospheric H_2O (Dubey et al., 1997). According to Table 5, the first reaction pathway produces nitrates via R4-R7-R8 with 2/3 of the O atoms coming from NO_2, 1/6 from O_3 and 1/6 from H_2O, while the second produces nitrates via R6 with 2 out of 3 O atoms coming from NO_2 and 1/3 from OH (e.g., Michalski et al., 2003). Using these proportions with the Alberta $\Delta^{17}O$ values of p-NO_3^- and HNO_3 in weighted averages allows us to make a rough estimation of the maximum and minimum $\Delta^{17}O$ values of NO_2 oxidized to nitrates in the air masses sampled. The calculations assume the O from O_3 contributes a signal of ~39 ‰ as

was recently measured (Vicars et al., 2014) and that $\Delta^{17}O$ of OH and H_2O are zero. The estimated NO_2 $\Delta^{17}O$ values for fall-winter (34-45 ‰ daytime, 25-36 ‰ nighttime) and for summer (25-34 ‰ for daytime; 15-24 ‰ for nighttime) represent the extremes assuming daytime oxidation takes place 100 % through the OH pathway and nighttime oxidation takes place entirely through the N_2O_5 pathway. One should keep in mind that the Alberta results are for nitrates collected during multi-week sampling periods. Each nitrate sample therefore contains *a priori* a mixture of O from the pathways operating during daytime (R6) and nighttime (R4-R7-R8). Assuming a 50 % contribution from each pathway for summer, we generate values ranging from 20 to 29 ‰. Alternatively, assuming domination of the N_2O_5 pathway during winter (90 %; Michalski et al., 2014), the range is 26-37 ‰. Fall and spring values should fit between these summer and winter estimated ranges. The estimated NO_2 $\Delta^{17}O$ ranges indicate that the potential parent NO_2 had a smaller ^{17}O anomaly than O_3 (39 ‰; Vicars and Savarino, 2014) or NO_2 in isotopic equilibrium with O_3 alone (45 ‰; Michalski et al., 2014) in all possible scenarios.

Two mechanisms could be responsible for the $\Delta^{17}O$ differences between these estimates and NO_2 in isotopic equilibrium with O_3. One is the competition of R3 with R2 in oxidizing NO to NO_2, since RO_2 will decrease the $\Delta^{17}O$ values relative to an ozone-only equilibrium. The relative reaction rates of R2 and R3 have previously been presumed to control the NO_2 isotopic composition (e.g., Alexander et al., 2009) based on the assumption of isotopic steady state. A larger contribution of RO_2 is expected in the NO_2 precursors for summer relative to winter, since biogenic VOCs that are major sources of RO_2 radicals are much higher in the summer (e.g., Fuentes and Wang, 1999). This suggestion is consistent with the lower $\Delta^{17}O$ ranges in summer reported here. A second possibility is that the nitrates were formed from some NO_x that did not reach isotopic steady state with O_3, retaining some of its original signature (assumed to be $\Delta^{17}O$=0 ‰). Most studies have assumed that isotopic steady state is established between O_3 and NO_2 within a few minutes after emission of NO_x from a combustion source – or at least, that nitrate formation is negligible before NO_x isotopic equilibrium is reached. However, recent modeling by Michalski et al. (2014) suggests that isotopic equilibration of NO_x with O_3 could take several minutes up to a few hours at the relatively low O_3 concentrations in rural Alberta. At the measured average wind speeds on site of 8-19 km h^{-1}, transit times from the nearest sources to observation sites are estimated to be 9-55 minutes. While the fraction of NO_x converted to nitrate in this transit time may be small, these are large sources of NO_x in an area with very low background nitrates. For example, a plume containing 10 nmol mol^{-1} of NO_2 mixing with background air with 0.1 pmol mol^{-1} of OH (Howell et al., 2014) would produce HNO_3 via R6 at a rate of 0.011 μg m^{-3} min^{-1} of NO_3^--N at T = 7 °C (Burkholder et al., 2015), or an equivalent amount of a typical nitrate sample in 10 minutes (Table SM-1). Even if equilibration with O_3 is established within a few minutes, the nitrate produced in the interim can constitute a substantial fraction of the sample collected nearby. Therefore, the nitrates measured at our sites may partly derive from NO_x that had not yet reached isotopic steady state with O_3. These two mechanisms are not exclusive and could both contribute to lower NO_x, and therefore nitrate, $\Delta^{17}O$ values.

An additional piece of evidence suggests that the NO_x plumes themselves, rather than ambient conditions, are the source of low-$\Delta^{17}O$ nitrates in these samples. There is a strong correlation between the total nitrate $\Delta^{17}O$ values and the maturity of the plume as expressed by the NO_2 concentration divided by sum of HNO_3 and p-NO_3^- concentrations (Fig. 5). This observation is consistent with the unequilibrated NO_2 hypothesis. However, it does not rule out the possible contribution of RO_2, since VOC releases from the NO_x sources could lead to elevated RO_2 concentrations in the plume.

4.2 Causes of shifts in HNO_3 to p-NO_3^- isotopic differences

A challenging question is why do the HNO_3 to p-NO_3^- isotopic differences shift seasonally (Fig. 3)? One factor that may influence the relationship between HNO_3 and p-NO_3^- is mass-dependent isotopic equilibrium between NH_4NO_3 and HNO_3 (R10); however, this mechanism would result in higher $\delta^{18}O$ in p-NO_3^- and unchanged $\Delta^{17}O$ values and, therefore, cannot be solely responsible for any of the observed patterns (Fig. 3). Alternately, the trend for cold months (trend *i*) could be due to the fact that the heterogeneous N_2O_5 pathway is likely to produce more p-NO_3^- than HNO_3(g), which would result in a higher contribution from ozone and explain why $\delta^{18}O$ and $\Delta^{17}O$ values are both higher in p-NO_3^-. A previous study addressing why p-NO_3^- on coarse particles is more enriched than on fine particles invoked a similar explanation (Patris et al., 2007).

For some of the spring and summer samples, both $\delta^{18}O$ and $\Delta^{17}O$ values were lower in p-NO_3^- than in HNO_3 (trend *iv*), therefore the mechanism above cannot dominate the fractionation; nor can a mass-dependent process be responsible. We suggest a different fractionation process because HNO_3 dry deposits to surfaces more rapidly than p-NO_3^- (Zhang et al., 2009; Benedict et al., 2013), which would create the discussed isotopic shifts in the situation where NO_2 has low $\Delta^{17}O$ values in a fresh plume. The first nitrates formed in the plume shortly after emission from the NO_x source have low $\delta^{18}O$ and $\Delta^{17}O$ values, either because NO_x has not yet reached isotopic steady state with O_3 or because it reacted with ^{17}O-poor RO_2 present in the plume due to VOC emissions. Those nitrates that form as p-NO_3^- or that partition to p-NO_3^- remain in the plume for longer than HNO_3, which is removed from the plume rapidly upon contact with vegetation or other surfaces. As the plume travels, the NO_x becomes more enriched, and the newly formed nitrates take on higher $\delta^{18}O$ and $\Delta^{17}O$ values. However, p-NO_3^- collected further downwind will derive from a mixture of low-$\delta^{18}O$ and -$\Delta^{17}O$ p-NO_3^- formed earlier, plus high-$\delta^{18}O$ and -$\Delta^{17}O$ p-NO_3^- formed more recently, while HNO_3 will have a larger proportion formed more recently and will therefore have higher $\delta^{18}O$ and $\Delta^{17}O$ values. The fact that we find the lowest isotopic values in summer p-NO_3^- samples collected from various anthropogenic sources at distances less than 16 km supports this suggestion (Table 1).

The above two mechanisms that we propose to explain the shifts in HNO_3 to p-NO_3- isotopic differences between cold and warm sampling periods – differential N_2O_5 contribution resulting in higher $\Delta^{17}O$ values in p-NO_3^- than in HNO_3, and differential deposition resulting in lower $\Delta^{17}O$ values in p-NO_3 – would essentially compete against each other, with local conditions and chemistry influencing the results. In winter, when the N_2O_5 pathway is most important, the first mechanism dominates, as supported by the observation that p-NO_3^- concentrations are higher during that season (trend *i*). Conversely, in summer, when the N_2O_5 pathway is less important and dry deposition is likely faster due to absence of snow cover, higher surface wetness and high leaf areas, the second mechanism is more important (trend *iv*). The local reactant concentrations, wind speeds and radiative fluxes (which control the time to reach isotopic equilibrium) would also be factors in the second mechanism. We find intermediate trends (*ii, iii*) in the transitional seasons, as expected. In addition to these non-mass-dependent fractionation processes, mass-dependent fractionation in formation and loss of nitrate likely contributes to the observed $\delta^{18}O$ differences. For instance, kinetic fractionation may be involved in the production of trend *iii*.

In summary, examining the isotopic relationship of HNO_3 to p-NO_3^- (Fig. 3), reveals the complexity of anthropogenic NOx oxidation mechanisms. The lower p-NO_3^- isotopic values relative to the HNO_3 values during warm months may reflect differential removal rates from plumes containing NO_2 temporarily low in ^{17}O.

4.3 - Low $\delta^{18}O$ and $\Delta^{17}O$ trends in global w- and p-NO_3^- - Implications for polluted air masses

Atmospheric nitrates measured in central and southern Alberta were sampled downwind of well-identified anthropogenic sources to verify the potential role of emitted NO_x isotopic signals through to final nitrate isotopic ratios (primarily N isotopes; see Savard et al., 2017). As expected, the measured oxygen isotopes of the various nitrate groups are consistent with exchange with O_3 and oxidation through the well-known OH and N_2O_5 oxidation paths. However, NO_2 not in isotopic equilibrium with O_3, and/or NO reacted with RO_2 may have significantly influenced the overall results. Co-contaminants in the emissions and sampling plumes at short distances from the sources may have favoured these two mechanisms, and quantifying RO_2 and/or HO_2 would help distinguish between the two mechanisms. Meanwhile, our results raise the question: are these overall effects observable in triple oxygen isotopes of nitrates from other polluted sites?

The full $\Delta^{17}O$ and $\delta^{18}O$ ranges for p-NO_3^-, w-NO_3^- and HNO_3 (between 13.8 and 20.5 ‰, 48.4 and 83.2 ‰; Table 4) compare well with the isotopic ranges obtained for bulk deposition NO_3^- samples collected downwind from oil sands mining operations in the lower Athabasca region farther north in Alberta (Proemse et al., 2013). Moreover, the isotopic values in cold and warm months delineated here essentially overlap with the data sets of winter and summer from the lower Athabasca region (Fig. 6). This correspondence exists despite the slightly different climatic conditions (Fig. SM-1), and very different sampling methods (bulk/throughfall deposition samples using open ion exchange resin collectors, vs. wind sector-specific active sampling on filters and precipitation-only collectors). Notably, many points carry relatively low $\delta^{18}O$ and $\Delta^{17}O$ values.

Previous work in the Athabasca region reported very low $\delta^{18}O$ and near-zero $\Delta^{17}O$ values for p-NO_3^- sampled directly within oil-sands industrial stacks, i.e., in the emissions measured in-stack and diluted with ambient air (Proemse et al., 2012). These values are very close to those of O_2. Similar isotopic signatures are very likely produced in source emissions of NO_x in the studied Edmonton and Vauxhall areas (e.g., CFPP, gas compressors, industries). This source signature may persist into p-NO_3 collected close to the sources. Within the first few hours in the atmosphere (less, in polluted areas), the NO_x $\delta^{18}O$ and $\Delta^{17}O$ values rapidly increase due to isotope exchange with O_3 (R2, R3, R5 and O_3 formation, Table 5; Michalski et al., 2014) and reach isotopic equilibrium. Though the e-folding lifetime for NO_x oxidation to nitrates may be longer than these few hours, depending on the NO_x/VOC ratio, only a fraction of the oxidized source NO_x will create a measureable contribution to the ambient nitrate where the background air is very low in nitrate. This is likely the case in the oil sands region, where Proemse et al. (2013) reported the lowest $\Delta^{17}O$ values within 12 km of the emission sites, and where direct stack emissions of p-NO_3^- were ~5000 times lower than NO_x emissions (Wang et al., 2012).

In a methodological test study, we obtained low values for w-NO_3^- sampled near a high traffic volume highway in Ontario, Canada (Smirnoff et al., 2012). Low $\delta^{18}O$ and $\Delta^{17}O$ values in atmospheric nitrates during warm months (65 and 20 ‰ or less,

respectively) have been reported for other parts of the world as well (Table 4). Authors of these studies have invoked peroxy radicals to account for low $\delta^{18}O$ values in w-NO_3^- from a polluted city (Fang et al., 2011), in p-NO_3^- from Taiwan collected partly from air masses influenced by pollutants (Guha et al., 2017) and from a polluted coastal site in California (Michalski et al., 2004; Patris et al., 2007; Table 4). However, sampling in these three other regions did not use collection restricted to air masses transported from targeted anthropogenic sources. So uncertainties persist regarding the ultimate sources of nitrates with low isotopic values.

Although a few low values are also reported for seemingly non-polluted areas of the Arctic and Antarctic regions (unknown cause; Morin et al., 2008; Morin et al., 2009) and of coastal California (Patris et al., 2007), the information from the literature integrated with the interpretation proposed for the Alberta low $\delta^{18}O$ and $\Delta^{17}O$ values in summer nitrates may reflect the involvement of air masses that include nitrates from oxidation of NO_2 with light isotopes in plumes. In such cases, while not ruling out a higher contribution from RO_2 oxidation of NO, it is also possible that significant portions of the collected nitrate were formed before the NO_x-O_3 isotopic equilibrium was reached (see Section 4.1). Keeping in mind that other hydrocarbon and halogen pathways may play a role in determining the isotopic nitrate characteristics in other parts of the world, we propose that, in general, the warm-periods isotopic ranges appear to be lower in polluted areas. Given these points, our nitrate $\delta^{18}O$ and $\Delta^{17}O$ may reflect relative proximity to anthropogenic N emitters in general. Further research work on plume NO_x to nitrates chemical mechanisms may help to validate this suggestion. In the future, the assumption of NO_x isotopic steady state with O_3 should be explored, given recent findings (Michalski et al., 2014), the critical importance of NO_x isotope characteristics on resulting nitrate isotopic values (Alexander et al., 2009), and the suggestion regarding the evolution of NO_x-NO_3^- signals in fresh anthropogenic plumes (present study).

5 Conclusion

The HNO_3, w-NO_3 and p-NO_3 from anthropogenic sources in central and southern Alberta, simultaneously collected with wind sector-based conditional sampling systems produced $\delta^{18}O$ and $\Delta^{17}O$ trends confirming the previous contention that regional ambient conditions (e.g., light intensity, oxidant concentrations, RH, temperature) dictate the triple isotopic characteristics and oxidation pathways of nitrates.

The gaseous form of nitrate (HNO_3) having distinct isotopic characteristics relative to the wet and particulate forms implies that understanding nitrate formation and loss requires characterizing the nitrate species individually. Particulate-NO_3^- in these samples generally shows higher $\delta^{18}O$ and $\Delta^{17}O$ values than HNO_3 in the fall-winter period as the heterogeneous N_2O_5 pathway favours the production of p-NO_3^-. In contrast, HNO_3 has higher $\delta^{18}O$ and $\Delta^{17}O$ values during warm periods, which we propose is due to faster dry deposition rates relative to p-NO_3^- in the event that low-$\Delta^{17}O$ NO_2 is oxidized in the plume. The mechanisms conferring nitrate with relatively low isotopic values, whether oxidation before NO_x-O_3 equilibrium is reached or higher contributions from RO_2, are likely to be observed in anthropogenic polluted air masses. An interesting deduction arising from this interpretation and from a comparison with nitrate isotopes from other polluted areas of the world is that relatively low $\delta^{18}O$ and $\Delta^{17}O$ values may reflect nitrates produced from undifferentiated anthropogenic NO_x emissions.

Future research should explore the assumption of NO_x isotopic equilibration with O_3, given the critical importance of NO_x isotopes on resulting nitrate isotopic values. More field sampling, including additional on-site oxidant data, and state-of-the-art isotopic analyses of all tropospheric nitrate species as well as NO_x are required for refining our understanding of atmospheric nitrate worldwide. This endeavour is fundamental for developing effective emission-reduction strategies towards improving future air quality.

Acknowledgements. The authors are grateful for the technical support provided by Marie-Christine Simard and Jade Bergeron of the Geological Survey of Canada, and by Syed Iqbal, Rachel Mintz, Daniel McLennan, Matthew Parsons, Mike Shaw Amy Hou of Environment and Climate Change Canada; and for the constructive pre-submission review by Drs. Geneviève Bordeleau from the Geological Survey of Canada, and Felix Vogel and Jason O'Brien from ECCC. This research has been financially supported by the Clean Air Regulatory Agenda of Environment and Climate Change Canada, and the Environmental Geoscience program of Natural Resources Canada (NRCan contribution number: 20170310). The first author dedicates this research article to Pauline Durand for her support.

References

Alexander, B., Hastings, M. G., Allman, D. J., Dachs, J., Thornton, J. A., and Kunasek, S. A.: Quantifying atmospheric nitrate formation pathways based on a global model of the oxygen isotopic composition (δ17O) of atmospheric nitrate, Atmospheric Chemistry and Physics, 9, 5043-5056, 2009.

Anlauf, K. G., Fellin, P., Wiebe, H. A., Schiff, H. I., Mackay, G. I., Braman, R. S., and Gilbert, R.: A comparison of three methods for measurement of atmospheric nitric acid and aerosol nitrate and ammonium, Atmospheric Environment (1967), 19, 325-333, 10.1016/0004-6981(85)90100-3, 1985.

Anlauf, K. G., Wiebe, H. A., and Fellin, P.: Characterization of Several Integrative Sampling Methods for Nitric Acid, Sulphur Dioxide and Atmospheric Particles, Journal of the Air Pollution Control Association, 36, 715-723, 10.1080/00022470.1986.10466107, 1986.

Appel, B. R., Tokiwa, Y., and Haik, M.: Sampling of nitrates in ambient air, Atmospheric Environment (1967), 15, 283-289, 10.1016/0004-6981(81)90029-9, 1981.

Benedict, K. B., Carrico, C. M., Kreidenweis, S. M., Schichtel, B., Malm, W. C., and Collett Jr, J. L.: A seasonal nitrogen deposition budget for Rocky Mountain National Park, Ecological Applications, 23, 1156-1169, 10.1890/12-1624.1, 2013.

Brown, S. S., Ryerson, T. B., Wollny, A. G., Brock, C. A., Peltier, R., Sullivan, A. P., Weber, R. J., Dubé, W. P., Trainer, M., Meagher, J. F., Fehsenfeld, F. C., and Ravishankara, A. R.: Variability in nocturnal nitrogen oxide processing and its role in regional air quality, Science, 311, 67-70, 10.1126/science.1120120, 2006.

Cheng, I., and Zhang, L.: Long-term air concentrations, wet deposition, and scavenging ratios of inorganic ions, HNO3, and SO2 and assessment of aerosol and precipitation acidity at Canadian rural locations, Atmospheric Chemistry and Physics, 17, 4711-4730, 10.5194/acp-17-4711-2017, 2017.

Coplen, T. B., Böhlke, J. K., and Casciotti, K.: Rapid Commun. Mass Spectrom., 18, 245, 2004.

Dahal, B., and Hastings, M. G.: Technical considerations for the use of passive samplers to quantify the isotopic composition of NO x and NO 2 using the denitrifier method, Atmospheric Environment, 143, 60-66, 2016.

Dubey, M. K., Mohrschladt, R., Donahue, N. M., and Anderson, J. G.: Isotope specific kinetics of hydroxyl radical (OH) with water (H2O): Testing models of reactivity and atmospheric fractionation, Journal of Physical Chemistry A, 101, 1494-1500, 1997.

Elliott, E. M., Kendall, C., Boyer, E. W., Burns, D. A., Lear, G. G., Golden, H. E., Harlin, K., Bytnerowicz, A., Butler, T. J., and Glatz, R.: Dual nitrate isotopes in dry deposition: Utility for partitioning NO x source contributions to landscape nitrogen deposition, Journal of Geophysical Research: Biogeosciences, 114, 10.1029/2008JG000889, 2009.

Environment and Climate Change Canada; Air Pollutant Emission Inventory Online Data Query: http://www.ec.gc.ca/inrp-npri/donnees-data/ap/index.cfm?lang=En, access: accessed 2016/12/15, 2016.

Environment and Climate Change Canada; Canadian Air and Precipitation Monitoring Network (CAPMoN): http://donnees.ec.gc.ca/data/air/monitor/monitoring-of-atmospheric-precipitation-chemistry/major-ions/, 2018a.

Environment and Climate Change Canada; National Pollutant Release Inventory: https://www.canada.ca/en/environment-climate-change/services/national-pollutant-release-inventory/tools-resources-data.html, 2018b.

Erisman, J. W., and Fowler, D.: Oxidized and reduced nitrogen in the atmosphere, Knowledge for Sustainable Development, An Insight into the Encyclopedia of Life Support Systems, Volumes I, II, III, UNESCO Publishing-Eolss Publishers, Oxford, UK, 2003.

Fang, Y. T., Koba, K., Wang, X. M., Wen, D. Z., Li, J., Takebayashi, Y., Liu, X. Y., and Yoh, M.: Anthropogenic imprints on nitrogen and oxygen isotopic composition of precipitation nitrate in a nitrogen-polluted city in southern China, Atmospheric Chemistry and Physics, 11, 1313-1325, 10.5194/acp-11-1313-2011, 2011.

Fuentes, J. D., and Wang, D.: On the seasonality of isoprene emissions from a mixed temperate forest, Ecological Applications, 9, 1118-1131, 10.1890/1051-0761(1999)009[1118:OTSOIE]2.0.CO;2, 1999.

Guha, T., Lin, C. T., Bhattacharya, S. K., Mahajan, A. S., Ou-Yang, C. F., Lan, Y. P., Hsu, S. C., and Liang, M. C.: Isotopic ratios of nitrate in aerosol samples from Mt. Lulin, a high-altitude station in Central Taiwan, Atmospheric Environment, 154, 53-69, 10.1016/j.atmosenv.2017.01.036, 2017.

Hastings, M. G., Sigman, D. M., and Lipschultz, F.: Isotopic evidence for source changes of nitrate in rain at Bermuda, Journal of Geophysical Research D: Atmospheres, 108, ACH 22-21 - ACH 22-12, 2003.

IPCC; Fifth Assessment Report (AR5): https://www.ipcc.ch/report/ar5/, access: September 2017, 2013.

Johnston, J. C., and Thiemens, M. H.: The isotopic composition of tropospheric ozone in three environments, Journal of Geophysical Research Atmospheres, 102, 25395-25404, 1997.

Kaiser, J., Hastings, M. G., Houlton, B. Z., Röckmann, T., and Sigman, D. M.: Triple oxygen isotope analysis of nitrate using the denitrifier method and thermal decomposition of N2O, Analytical Chemistry, 79, 599-607, 10.1021/ac061022s, 2007.

Kane, S. M., Caloz, F., and Leu, M. T.: Heterogeneous uptake of gaseous N2O5 by (NH4)2SO4, NH4HSO4, and H2SO4 aerosols, Journal of Physical Chemistry A, 105, 6465-6470, 10.1021/jp010490x, 2001.

Keck, L., and Wittmaack, K.: Effect of filter type and temperature on volatilisation losses from ammonium salts in aerosol matter, Atmospheric Environment, 39, 4093-4100, 10.1016/j.atmosenv.2005.03.029, 2005.

Kendall, C., Elliott, E. M., and Wankel, S. D.: Tracing Anthropogenic Inputs of Nitrogen to Ecosystems, in: Stable Isotopes in Ecology and Environmental Science: Second Edition, 375-449, 2007.

Lavoie, G. A., Heywood, J. B., and Keck, J. C.: EXPERIMENTAL AND THEORETICAL STUDY OF NITRIC OXIDE FORMATION IN INTERNAL COMBUSTION ENGINES, M, I.T.-Dept Mech Eng-Fluid Mechanics Laboratory Publ 69-10, 1969.

Liang, M. C., and Yung, Y. L.: Sources of the oxygen isotopic anomaly in atmospheric N<inf>2</inf>O, Journal of Geophysical Research Atmospheres, 112, 10.1029/2006JD007876, 2007.

McIlvin, M. R., and Altabet, M. A.: Chemical conversion of nitrate and nitrite to nitrous oxide for nitrogen and oxygen isotopic analysis in freshwater and seawater, Analytical Chemistry, 77, 5589-5595, 2005.

Michalski, G., Scott, Z., Kabiling, M., and Thiemens, M. H.: First measurements and modeling of Δ17O in atmospheric nitrate, Geophysical Research Letters, 30, 14-11, 2003.

Michalski, G., Meixner, T., Fenn, M., Hernandez, L., Sirulnik, A., Allen, E., and Thiemens, M.: Tracing Atmospheric Nitrate Deposition in a Complex Semiarid Ecosystem Using Δ17O, Environmental Science and Technology, 38, 2175-2181, 10.1021/es034980+, 2004.

Michalski, G., Bhattacharya, S. K., and Girsch, G.: NOx cycle and the tropospheric ozone isotope anomaly: An experimental investigation, Atmospheric Chemistry and Physics, 14, 4935-4953, 10.5194/acp-14-4935-2014, 2014.

Morin, S., Savarino, J., Bekki, S., Gong, S., and Bottenheim, J. W.: Signature of Arctic surface ozone depletion events in the isotope anomaly (Δ17O) of atmospheric nitrate, Atmospheric Chemistry and Physics, 7, 1451-1469, 2007.

Morin, S., Savarino, J., Frey, M. M., Yan, N., Bekki, S., Bottenheim, J. W., and Martins, J. M. F.: Tracing the origin and fate of NOx in the arctic atmosphere using stable isotopes in nitrate, Science, 322, 730-732, 10.1126/science.1161910, 2008.

Morin, S., Savarino, J., Frey, M. M., Domine, F., Jacobi, H. W., Kaleschke, L., and Martins, J. M. F.: Comprehensive isotopic composition of atmospheric nitrate in the Atlantic Ocean boundary layer from 65°S to 79°N, Journal of Geophysical Research Atmospheres, 114, 10.1029/2008JD010696, 2009.

Morino, Y., Kondo, Y., Takegawa, N., Miyazaki, Y., Kita, K., Komazaki, Y., Fukuda, M., Miyakawa, T., Moteki, N., and Worsnop, D. R.: Partitioning of HNO<inf>3</inf> and particulate nitrate over Tokyo: Effect of vertical mixing, Journal of Geophysical Research Atmospheres, 111, 10.1029/2005JD006887, 2006.

Patris, N., Cliff, S. S., Quinn, P. K., Kasem, M., and Thiemens, M. H.: Isotopic analysis of aerosol sulfate and nitrate during ITCT-2k2: Determination of different formation pathways as a function of particle size, Journal of Geophysical Research Atmospheres, 112, 10.1029/2005JD006214, 2007.

Proemse, B. C., Mayer, B., Chow, J. C., and Watson, J. G.: Isotopic characterization of nitrate, ammonium and sulfate in stack PM 2.5 emissions in the Athabasca Oil Sands Region, Alberta, Canada, Atmospheric Environment, 60, 555-563, 10.1016/j.atmosenv.2012.06.046, 2012.

Proemse, B. C., Mayer, B., Fenn, M. E., and Ross, C. S.: A multi-isotope approach for estimating industrial contributions to atmospheric nitrogen deposition in the Athabasca oil sands region in Alberta, Canada, Environmental Pollution, 182, 80-91, 10.1016/j.envpol.2013.07.004, 2013.

Randles, R. H., and Wolfe, D. A.: Introduction to the theory of nonparametric statistics, Wiley New York, 1979.

Rolph, G. D.; Real-time Environmental Applications and Display sYstem (READY): http://www.ready.noaa.gov, access: January, 2017.

Savard, M. M., Cole, A., Smirnoff, A., and Vet, R.: δ15N values of atmospheric N species simultaneously collected using sector-based samplers distant from sources – Isotopic inheritance and fractionation, Atmospheric Environment, 162, 11-22, 10.1016/j.atmosenv.2017.05.010, 2017.

Savarino, J., Kaiser, J., Morin, S., Sigman, D. M., and Thiemens, M. H.: Nitrogen and oxygen isotopic constraints on the origin of atmospheric nitrate in coastal Antarctica, Atmospheric Chemistry and Physics, 7, 1925-1945, 2007.

Savarino, J., Bhattacharya, S. K., Morin, S., Baroni, M., and Doussin, J. F.: The NO+ O3 reaction: A triple oxygen isotope perspective on the reaction dynamics and atmospheric implications for the transfer of the ozone isotope anomaly, Journal of Chemical Physics, 128, 10.1063/1.2917581, 2008.

Seinfeld, J. H., and Pandis, S. N.: Atmospheric chemistry and physics. Hoboken, NJ: Wiley, 2006.

Sickles Ii, J. E., Hodson, L. L., McClenny, W. A., Paur, R. J., Ellestad, T. G., Mulik, J. D., Anlauf, K. G., Wiebe, H. A., Mackay, G. I., Schiff, H. I., and Bubacz, D. K.: Field comparison of methods for the measurement of gaseous and particulate contributors to acidic dry deposition, Atmospheric Environment Part A, General Topics, 24, 155-165, 10.1016/0960-1686(90)90451-R, 1990.

Sickles Ii, J. E., Hodson, L. L., and Vorburger, L. M.: Evaluation of the filter pack for long-duration sampling of ambient air, Atmospheric Environment, 33, 2187-2202, 10.1016/S1352-2310(98)00425-7, 1999.

Sirois, A., and Fricke, W.: Regionally representative daily air concentrations of acid-related substances in Canada; 1983-1987, Atmospheric Environment Part A, General Topics, 26, 593-607, 10.1016/0960-1686(92)90172-H, 1992.

Sirois, A., and Vet, R.: The Precision of Precipitation Chemistry Measurements in the Canadian Air and Precipitation Monitoring Network (CAPMoN), Environmental Monitoring and Assessment, 57, 301-329, 10.1023/a:1006035129393, 1999.

Smirnoff, A., Savard, M. M., Vet, R., and Simard, M. C.: Nitrogen and triple oxygen isotopes in near-road air samples using chemical conversion and thermal decomposition, Rapid Communications in Mass Spectrometry, 26, 2791-2804, 10.1002/rcm.6406, 2012.

Spicer, C. W., Howes Jr, J. E., Bishop, T. A., Arnold, L. H., and Stevens, R. K.: Nitric acid measurement methods: An intercomparison, Atmospheric Environment (1967), 16, 1487-1500, 10.1016/0004-6981(82)90071-3, 1982.

Stein, A., Draxler, R., Rolph, G., Stunder, B., Cohen, M., and Ngan, F.: NOAA's HYSPLIT atmospheric transport and dispersion modeling system, Bulletin of the American Meteorological Society, 96, 2059-2077, 2015.

Stroud, C. A., Jonathan; Leiming, Zhang; Flagg, David; Makar, Paul: Atmospheric processes, Chapitre 2 - Draft version, in, Canadian smow Science Assessment, 2008.

Thiemens, M. H.: Mass-independent isotope effects in planetary atmospheres and the early solar system, Science, 283, 341-345, 10.1126/science.283.5400.341, 1999.

Tsunogai, U., Komatsu, D. D., Daita, S., Kazemi, G. A., Nakagawa, F., Noguchi, I., and Zhang, J.: Tracing the fate of atmospheric nitrate deposited onto a forest ecosystem in Eastern Asia using Δ17O, Atmospheric Chemistry and Physics, 10, 1809-1820, 2010.

Vicars, W. C., Bhattacharya, S. K., Erbland, J., and Savarino, J.: Measurement of the 17O-excess (δ 17O) of tropospheric ozone using a nitrite-coated filter, Rapid Communications in Mass Spectrometry, 26, 1219-1231, 10.1002/rcm.6218, 2012.

Vicars, W. C., Morin, S., Savarino, J., Wagner, N. L., Erbland, J., Vince, E., Martins, J. M. F., Lerner, B. M., Quinn, P. K., Coffman, D. J., Williams, E. J., and Brown, S. S.: Spatial and diurnal variability in reactive nitrogen oxide chemistry as reflected in the isotopic composition of atmospheric nitrate: Results from the CalNex 2010 field study, Journal of Geophysical Research Atmospheres, 118, 10567-10588, 10.1002/jgrd.50680, 2013.

Vicars, W. C., and Savarino, J.: Quantitative constraints on the 17O-excess (δ17O) signature of surface ozone: Ambient measurements from 50°N to 50°S using the nitrite-coated filter technique, Geochimica et Cosmochimica Acta, 135, 270-287, 10.1016/j.gca.2014.03.023, 2014.

Wang, X. L., Watson, J. G., Chow, J. C., Kohl, S. D., Chen, L. W. A., Sodeman, D. A., Legge, A. H., and Percy, K. E.: Measurement of Real-World Stack Emissions with a Dilution Sampling System, in: Developments in Environmental Science, 171-192, 2012.

Zel'dovich, Y. B.: The Oxidation of Nitrogen in Combustion and Explosions, Acta Physicochimica, 21, 577-628, 1946.

Zhang, L., Vet, R., O'Brien, J. M., Mihele, C., Liang, Z., and Wiebe, A.: Dry deposition of individual nitrogen species at eight Canadian rural sites, Journal of Geophysical Research Atmospheres, 114, 10.1029/2008JD010640, 2009.

Table 1. Settings and conditions for wind sector-based simultaneous sampling of atmospheric nitrates.

Site (coordinates)	**Sources**	**Distance** Km (mean)	**Sector** direction; opening	**Sampling** period;	**n**	**Avg T** (°C)	**Context**
Genesee (114.14° W, 53.31° N)	Coal-fired power plants	7–35	NW, 35°	30/09/2010 – 21/06/2011	6	11.7, 12.2, 5.5, -9.8, -0.9, 12.2	3 plants
Vauxhall (112.11° W, 50.06° N)	Gas compressors and cattle and swine feedlots	12-125+; 7.5-45+	W, 65°	25/10/2011 – 13/12/2011	3	2.6, 0.7,-3.5	65+ compressors; 200+ feedlots
Terrace Heights (113.44° W, 53.54° N)	Urban traffic	<1-15 (4)	W, 150°	24/07/2012 – 25/10/2012	4	20.3, 15.6, 7.9, -1.8	Park in residential area, 3.5 km east of downtown core
Fort Saskatchewan (113.14° W, 53.72° N)	Chemical industries and metal refining	3-7 (4)	NW, 88°	12/04/2013 – 06/09/2013	4	4.3, 15.7, 16.3, 17.7	Chemical plant and metal refinery largest NO_x sources; fertilizer plant largest NH_3 source
Fort Saskatchewan (113.14° W, 53.72° N)	Fertilizers plant and oil refinery	9-14 (11)	N, 27°	20/09/2013 – 20/01/2014	1	-8.1	Fertilizer plant largest NH_3 and NO_x source, oil refinery major NO_x source

N: number of sampling sessions. Avg T: average temperature during each of the consecutives sampling sessions.

Table 2. Isotopic reproducibility (modified median absolute deviation) established using 2 to 4 parallel active CAPMoN sampling setups in seven separate sampling periods, resulting in (n) total samples.

N compound (n)	**$\delta^{18}O$**	**$\delta^{17}O$**
Teflon filters p-NO_3^- (19)	2	1
Nylon filters HNO_3 (18)	1	0.7

Table 3. Average oxygen isotopic ratios (‰) for NO_3^- sampled as gas (HNO_3), w (precipitation) and p (particulate matter) relative to VSMOW.

Matrix	Gas	w	p	Gas	..w	..p
Source	**$\delta^{18}O$**			**$\Delta^{17}O$**		
Coal-fired power plants	69.7 (5)	66.1 (4)	70.7 (4)	25.1 (5)	25.4 (4)	26.6 (4)
Fertilizers plant & oil refinery	63.2 (1)	71.4 (1)	69.5 (1)	19.3 (1)	26.0 (1)	23.8 (1)
Chemical industries & metal refining	65.7 (4)	61.9 (2)	54.6 (4)	21.8 (4)	21.4 (2)	18.5 (4)
Gas compressors	65.0 (2)	-	63.1 (3)	24.5 (2)	-	26.4 (3)
City traffic	65.7 (3)	67.2 (2)	59.6 (3)	21.2 (3)	24.4 (2)	22.5 (3)
Mean	**66.8**	**66.0**	**62.6**	**23.0**	**24.3**	**23.4**

(n): number of sampling periods characterized

Table 4. Compilation of triple oxygen isotopic ranges obtained for atmospheric and emitted nitrates.

$\delta^{18}O$ (‰)	$\Delta^{17}O$ (‰)	Regional context	Location	Authors
HNO_3				
62.4-81.7	19.3-29.0	Various contaminated sites	Alberta, Canada	*This study*
p-NO_3^-				
43-62	20-27	Coast, Trinidad Head	California, USA	Patris et al. (2007)
78-92	29.8-35.0	High Arctic (Alert, Ellesmere Is.)	Nunavut, Canada	Morin et al. (2007)
62-112	19-43	Coast	Antarctica	Savarino et al. (2007)
15.6-36.0	-0.2 to 1.8	Oil-sands mining stacks, PM 2.5	Alberta, Canada	Proemse et al. (2012)
49-86	19-27	Coast (onboard sampling)	California, USA	Vicars et al. (2013)
10.8-92.4	2.7-31.4	Mt. Lulin, partly polluted air masses	Central Taiwan	Guha et al. (2017)
48.4-83.2	13.8-30.5	Various contaminated sites	Alberta, Canada	*This study*
w-NO_3^-				
66.3-84.0	20.2-36.0	Shenandoah National Park	Virginia, USA	Coplen et al. (2004)
70-90	20-30	Bi-monthly sampling across state	New England, USA	Kendall et al. (2007)
68-101	20.8-34.5	Rishiri Island, polluted air masses	Northern Japan	Tsunogai et al. (2010)
51.7-72.8	18.9-28.1	Highway traffic emissions	Ontario, Canada	Smirnoff et al. (2012)
35.0-80.7	15.7-32.0	Oil-sands mining (with some dry dep)	Alberta, Canada	Proemse et al. (2013)
57.4-74.4	19.2-30.1	Various contaminated sites	Alberta, Canada	*This study*
Undifferentiated and Bulk NO_3^-				
60-95	21-29	Polluted coastal area & Remote land	California, USA	Michalski et al. (2004)
57-79	22-32	High Arctic	Nunavut, Canada	Morin et al. (2008)
36-105	13-37	Marine boundary layer	65S to 79N Atlantic	Morin et al. (2009)
56.6-82.3*	16.7-30.2*	Various contaminated sites	Alberta, Canada	*This study*

Note: isotopic values rounded at unit are from published graphs (except for O values with actual precision at unit in Morin et al., 2007).
*Calculated using weighted averages of HNO_3 and p-NO_3 isotopic results.

5

Table 5. Main reactions producing atmospheric nitrates (Zel'dovich, 1946; Lavoie et al., 1969; Erisman and Fowler, 2003; Michalski et al., 2003; Morino et al., 2006; Morin et al., 2007; Stroud, 2008; Michalski et al., 2014) Reactions 1, 9-12 can occur any time.

Daytime - Summer	Nighttime - Winter
(R1) $O_2 + Q \rightarrow O + O + Q$; $N_2 + O \rightarrow NO + N$; $N + O_2 \rightarrow NO + O$	
(R2) $O + O_2 + M \rightarrow O_3$; $NO + O_3 \rightarrow NO_2 + O_2$	
(R3) $NO + RO_2 \rightarrow NO_2 + RO$	
	(R4) $NO_2 + O_3 \rightarrow NO_3 + O_2$
(R5) $NO_2 + h\nu$ (sunlight) $\rightarrow NO + O$	
(R6) $NO_2 + OH + M \rightarrow HNO_3 + M$	(R7) $NO_2 + NO_3^- \Leftrightarrow N_2O_5$
	(R8) $N_2O_5 + H_2O$(surface) $\rightarrow 2HNO_3$ (aq)*
(R9) $HNO_3(g) \Leftrightarrow HNO_3(aq)^* \rightarrow NO_3^-(aq)^* + H^+(aq)$	
(R10) $HNO_3(g) + NH_3(g) \Leftrightarrow NH_4NO_3(s)$	
(R11) $HNO_3(g) + CaCO_3(s) \rightarrow Ca(NO_3)_2(s) + HCO_3$	
(R12) $NO_3 + HC;(CH_3)_2S \rightarrow HNO_3 + products$	

*Q is a stable molecule of high energy; M is either O_2 or N_2; RO_2 stands for both HO_2 and alkyl peroxy. HC stand for hydrocarbons. *This aqueous nitrate may be on a particle.*

10

Table 6. Correlations of NO_3^- isotopic results (‰) with meteorological parameters and concentration (or ratio) of co-contaminants.

	Relative Humidity		Temperature		Daylight (fraction)		PM	SO_2	O_3	
	r	R^2	r	R^2	r	R^2	r	r	r	R^2
HNO_3										
$\delta^{18}O$	**0.8**	0.59	-0.4		-0.3		0.1	0.0	-0.29	
n	8		15		15		13	13	13	
$\Delta^{17}O$	0.6		**-0.5**	0.24	-0.4		0.4	0.3	-0.03	
n	8		15		15		13	13	13	
p-NO_3^-										
$\delta^{18}O$	**0.9**	0.79	**-0.6**	0.34	**-0.6**	0.35	0.1	0.5	**-0.61**	0.38
n	7		15		15		12	12	12	
$\Delta^{17}O$	**0.9**	0.73	**-0.6**	0.34	**-0.7**	0.44	0.0	0.5	-0.47	
n	7		15		15		12	12	12	

In **bold** are the significant correlation coefficients, equal or above the 95 % significance value

A

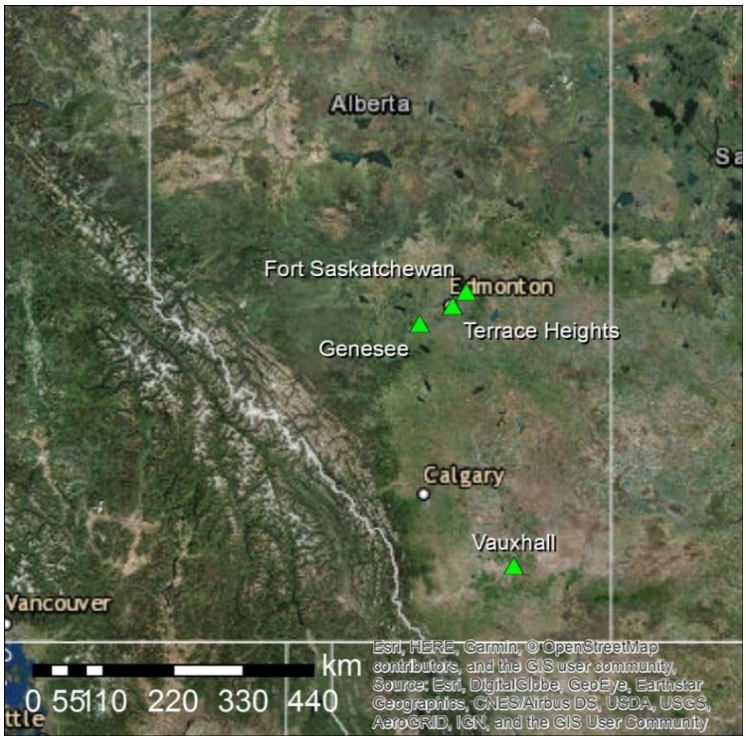

B

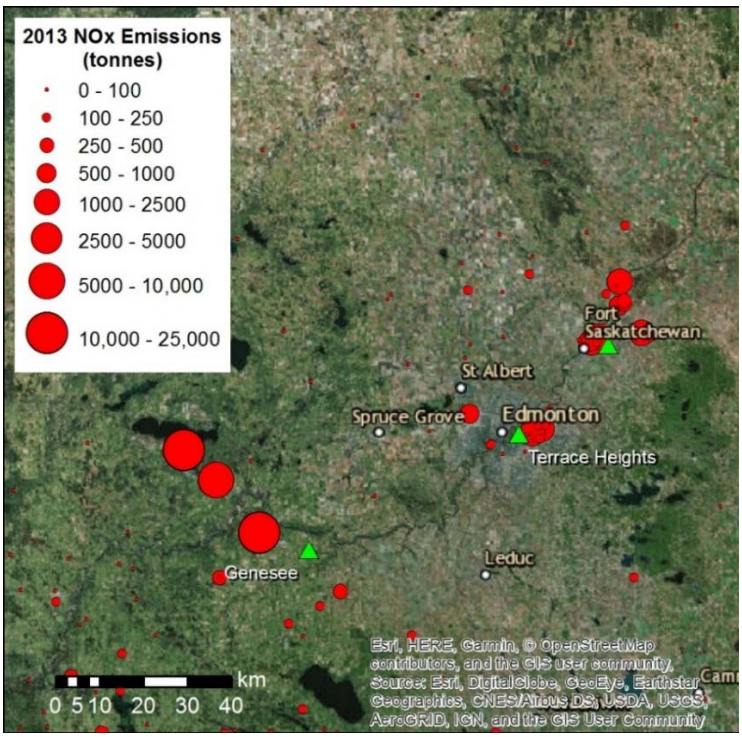

Figure 1. Aerial images showing sampling sites (green triangles) in central and southern Alberta (A), and in the greater Edmonton area (B), along with emissions of NO_x as tonnes of NO_2 reported to the National Pollutant Release Inventory for 2013 (Environment and Climate Change Canada, 2018b).

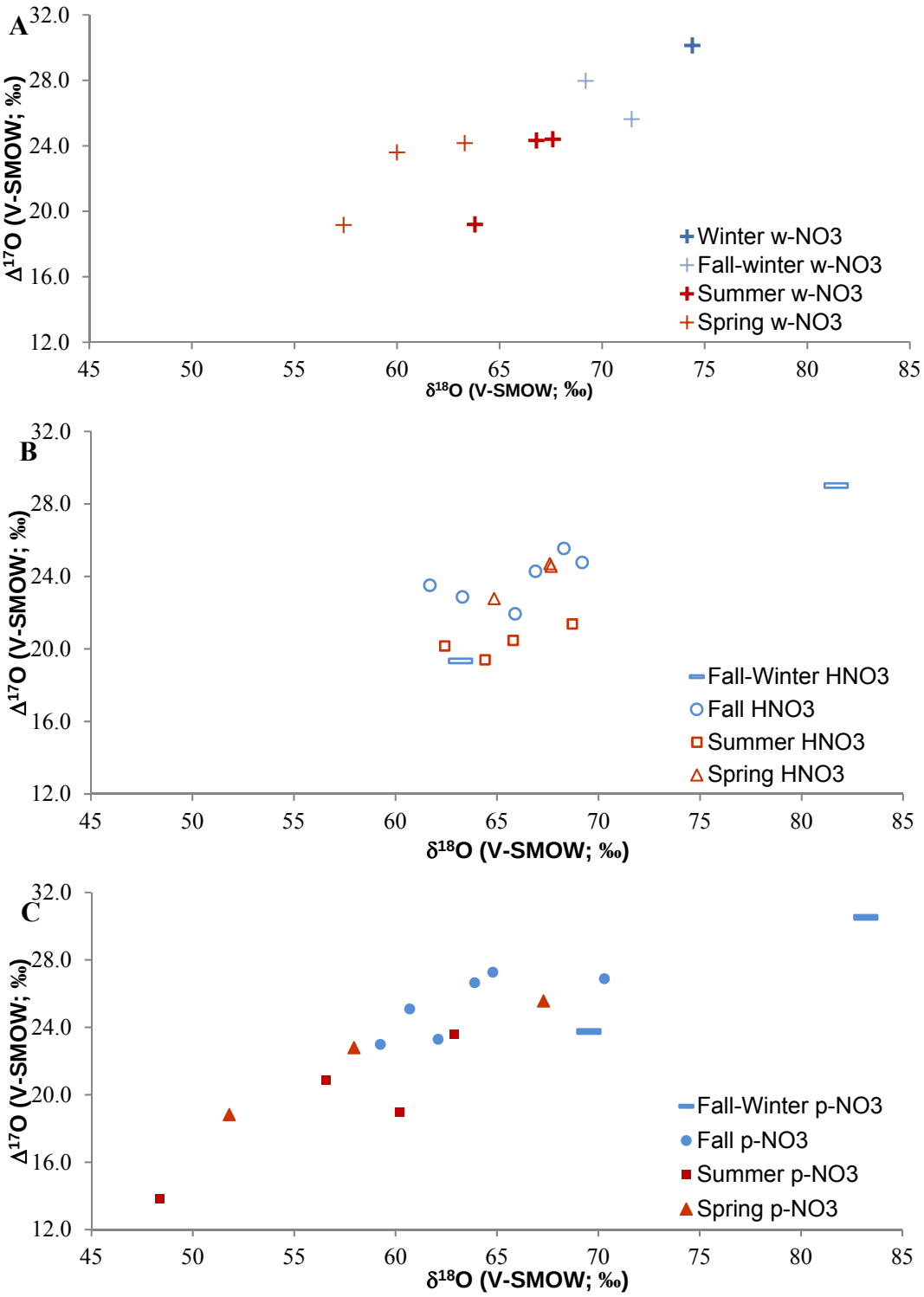

5 **Figure 2: Triple O isotopic results obtained for simultaneously collected atmospheric HNO_3 (A), w-NO_3^- (B) and p-NO_3^- (C), in Alberta, identified by sampling periods (cold months - blue; warm months - red).**

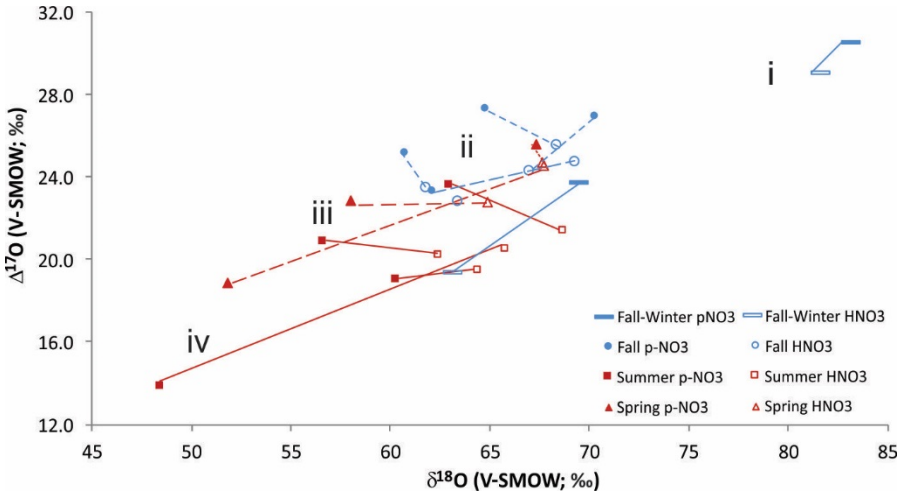

Figure 3: Line-connected $\delta^{18}O$ and $\Delta^{17}O$ values for simultaneously collected HNO_3 (empty symbols) and p-NO_3^- (solid symbols) from cold (blue) and warm (red) sampling periods.

5

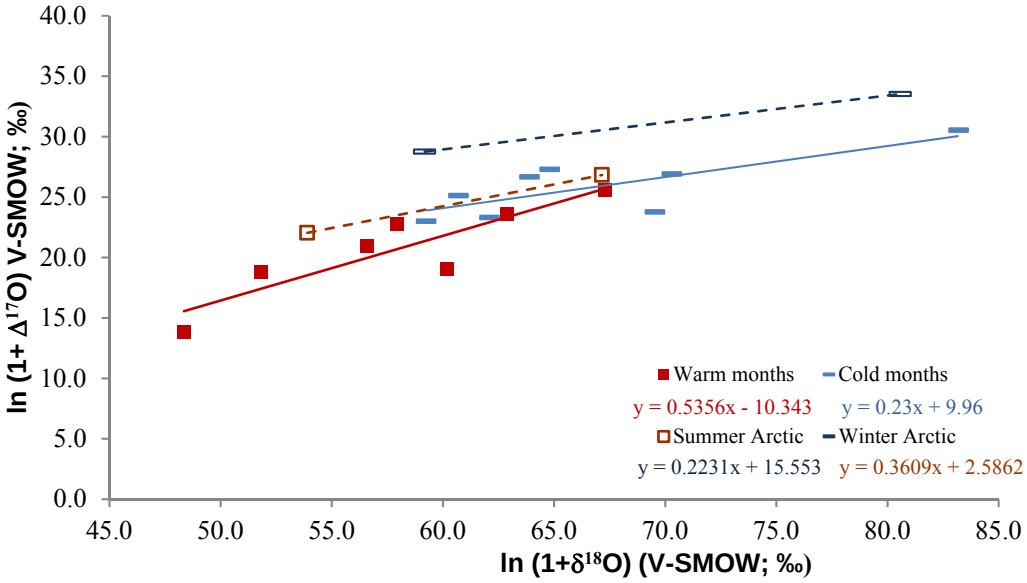

Figure 4: Isotopic results for p-NO_3^- identified by sampling periods (solid lines), compared with summer and winter trends obtained for Arctic sites (dashed lines; derived from ln (1+ δ) in Morin et al., 2008).

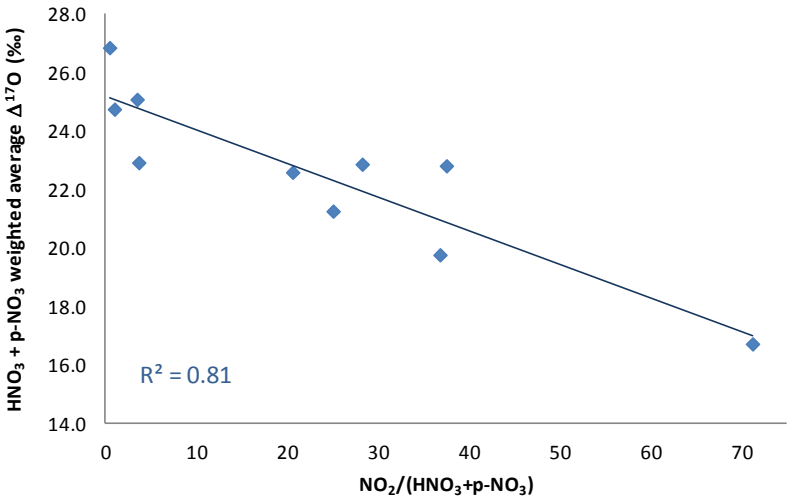

Figure 5: Weighted $\Delta^{17}O$ average for the sum of dry nitrates as a function of NO_2 concentration divided by p-NO_3 plus HNO_3 concentrations, a ratio indicative of the maturity of a plume.

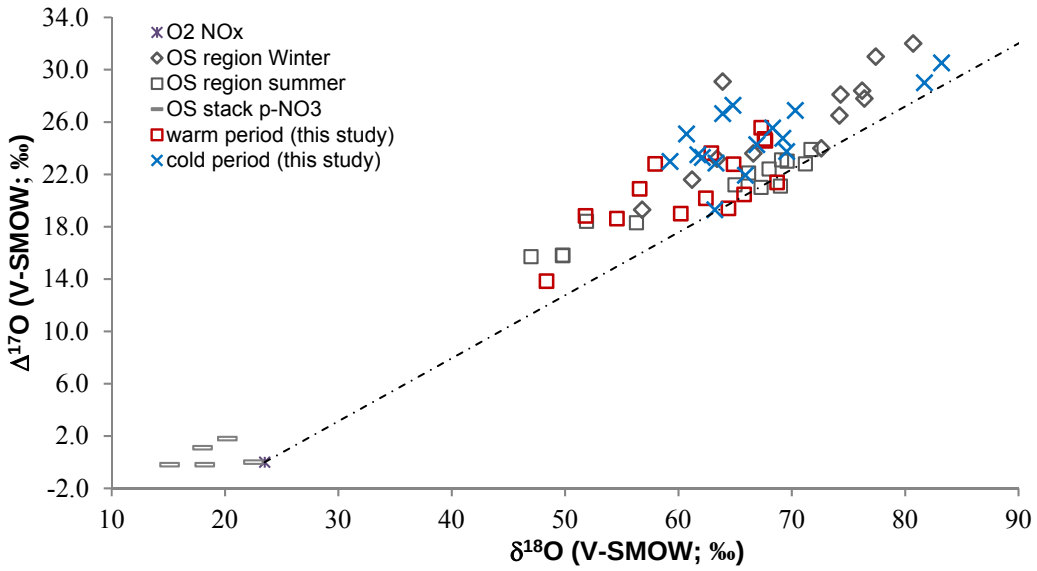

Figure 6: Isotopic ratios for atmospheric p-NO_3^-, w-NO_3^- and HNO_3 samples in cold and warm periods from central and southern Alberta (this study), compared with previously published winter and summer bulk and throughfall deposition samples from the oil sands (OS) region from northern Alberta (Proemse et al., 2013), and p-NO_3^- in-stack emissions data for an OS upgrader located in the same region (Proemse et al., 2012). The grey dotted line connects NO_x from theoretical combustion with O_2 isotopic composition and at isotopic equilibrium with tropospheric O_3 (Michalski et al., 2014).